Nanotoxicology

ISSN: 1743-5390 (Print) 1743-5404 (Online) Journal homepage: http://www.tandfonline.com/loi/inan20

Inflammation–coagulation response and thrombotic effects induced by silica nanoparticles in zebrafish embryos

Junchao Duan, Shuang Liang, Yang Yu, Yang Li, Lijing Wang, Zehao Wu, Yueyue Chen, Mark R. Miller & Zhiwei Sun

To cite this article: Junchao Duan, Shuang Liang, Yang Yu, Yang Li, Lijing Wang, Zehao Wu, Yueyue Chen, Mark R. Miller & Zhiwei Sun (2018) Inflammation–coagulation response and thrombotic effects induced by silica nanoparticles in zebrafish embryos, Nanotoxicology, 12:5, 470-484, DOI: 10.1080/17435390.2018.1461267

To link to this article: https://doi.org/10.1080/17435390.2018.1461267

NANOTOXICOLOGY
2018, VOL. 12, NO. 5, 470–484
https://doi.org/10.1080/17435390.2018.1461267

Taylor & Francis
Taylor & Francis Group

ARTICLE

Inflammation–coagulation response and thrombotic effects induced by silica nanoparticles in zebrafish embryos

Junchao Duan[a,b], Shuang Liang[a,b], Yang Yu[a,b], Yang Li[a,b], Lijing Wang[a,b], Zehao Wu[a,b], Yueyue Chen[a,b], Mark R. Miller[c] and Zhiwei Sun[a,b]

[a]Department of Toxicology and Sanitary Chemistry, School of Public Health, Capital Medical University, Beijing, P.R. China; [b]Beijing Key Laboratory of Environmental Toxicology, Capital Medical University, Beijing, P.R. China; [c]BHF Centre for Cardiovascular Science, Queens Medical Research Institute, The University of Edinburgh, Edinburgh, UK

ABSTRACT

Nowadays, nanotechnology environmental health and safety (nanoEHS) is gaining attention. We previously found that silica nanoparticles (SiNPs) could induce vascular endothelial damage. However, the subsequent toxicologic response to SiNPs-induced endothelial damage was still largely unknown. In this study, we explored the inflammation–coagulation response and thrombotic effects of SiNPs in endothelial cells and zebrafish embryos. For *in vitro* study, swollen mitochondria and autophagosome were observed in ultrastructural analysis. The cytoskeleton organization was disrupted by SiNPs in vascular endothelial cells. The release of proinflammatory and procoagulant cytokines including IL-6, IL-8, MCP-1, PECAM-1, TF and vWF, were markedly elevated in a dose-dependent manner. For *in vivo* study, based on the NOAEL for dosimetry selection, and using two transgenic zebrafish, Tg(mpo:GFP) and Tg(fli-1:EGFP), SiNPs-induced neutrophil-mediated inflammation and impaired vascular endothelial cells. With the dosage higher than NOAEL, SiNPs significantly decreased blood flow and velocity, exhibiting a blood hypercoagulable state in zebrafish embryos. The thrombotic effect was assessed by *o*-dianisidine staining, showed that an increasing of erythrocyte aggregation occurred in SiNPs-treated zebrafish. Microarray analysis was used to screen the possible genes for inflammation–coagulation response to SiNPs in zebrafish, and the JAK1/TF signaling pathway was further verified by qRT-PCR and Western blot assays. For in-deepth study, *il6st* was knocked down with specific morpholinos. The whole-mount *in situ* hybridization and qRT-PCR analysis showed that the expression *jak1* and *f3b* were attenuated in *il6st* knockdown groups. In summary, our data demonstrated that SiNPs could induce inflammation–coagulation response and thrombotic effects via JAK1/TF signaling pathway.

ARTICLE HISTORY
Received 14 October 2017
Revised 27 March 2018
Accepted 30 March 2018

KEYWORDS
Silica nanoparticles; inflammation–coagulation response; thrombotic effects; endothelial cells; zebrafish embryos

1. Introduction

Over the last decade, nanotechnology has grown exponentially for a diverse range of applications, including chemical industries, medicine, food sciences, biology, and electronics (Etheridge et al. 2013). For medicine applications, nanotechnology has the potential to bring benefits to drug delivery or gene therapy by improving biocompatibility, increasing uptake to target sites and changing pharmacokinetic profiles (Ilinskaya and Dobrovolskaia 2013). More than 50 nano-scale drugs are currently in clinical trials (Gabizon et al. 2014). Nanotechnology environmental health and safety (nanoEHS) is a research discipline that involves the study of the possible adverse health and biologic effects that nanomaterials may have on humans and environmental organisms and ecosystems (Nel et al. 2015). In recent years, nanoEHS is getting more and more attention. The application of nanotechnology in biomedical fields needs to be balanced by concerns about the potential health effects of nanomaterials.

Silica nanoparticles (SiNPs) are one of the most widely used engineered nanomaterials with unique physiochemical properties including high hydrophilicity, small size, large surface area with lots of hydroxyl radical (•OH), fantastic modification and good biocompatibility. In fact, the synthetic amorphous silica (SAS) is an engineered

CONTACT Zhiwei Sun zwsun@ccmu.edu.cn; Yueyue Chen ccccc1yy@ccmu.edu.cn Department of Toxicology and Sanitary Chemistry, School of Public Health, Capital Medical University, Beijing 100069, P.R. China

Supplemental data for this article can be accessed here.

nanomaterial that has been used as food additive more than half century. Nevertheless, SiNPs are the subject of new challenges regarding their potential adverse effects and safety evaluation (Hansen et al. 2008; Maynard 2014). SiNPs have been listed as a priority nanomaterial for toxicity evaluation by the Organization for Economic Co-operation and Development (OECD) (OECD 2010). In recent years, SiNPs are being designed as promising nanocarriers for drug delivery and cancer therapeutics via intravenous injection (Xu et al. 2016). Additionally, the diagnostic probe 'C-dots' encapsulated by SiNPs was approved by Food and Drug Administration (FDA) for Stage I human clinical trials (Benezra et al. 2011). In this way, SiNPs could interact with the blood components or vascular endothelial cells unavoidable. Thus, there is a clear need to address how SiNPs interact with the blood and vascular system.

Thrombosis is a major health concern globally, as a pathologic basis for cardiovascular disease and thrombotic complications. For example, the annual incidence for venous thromboembolism is in the order of 1/1000 (Rao, Kazzaz, and Knight 2015). Virchow's triad has demonstrated that the pathogenesis of thrombus formation involves detrimental actions on the vascular endothelium, hemodynamic control and hypercoagulability of blood (Solayar and Shannon 2014). Inflammation–coagulation response plays a key role in thrombus formation. However, few studies have addressed the inflammation–coagulation response and thrombus formation induced by nanoparticles. Silver nanoparticles have been shown to enhance thrombus formation in a surgical rat model (Jun et al. 2011). Furthermore, we demonstrated that SiNPs increased coagulation factor and platelet aggregation, resulting in pre-thrombotic state in rats (Jiang et al. 2015). In contrast, Yoshida et al. (2013) reported prolonged bleeding time and decreased platelet counts in mice following intranasal exposure to SiNPs. Further investigations are needed to clarify the potential adverse thrombotic effects of SiNPs and the biologic mechanisms involved.

Zebrafish (*Danio rerio*) have become an established model for genetic study, developmental biology, human diseases; and recently, for nanomaterials safety evaluation (Fako and Furgeson 2009; Hicken et al. 2011). Zebrafish are especially suitable for the study of hemostasis and thrombosis due to the conservation of virtually all coagulation factors in genomic sequence and the means to observe the circulation system without invasive methods (Weyand and Shavit 2014). The JAK signaling pathway is a critical to regulator inflammation, angiogenesis, vascular cell growth, immune response and other cellular processes (Murray 2007; Fang et al. 2013). Activation of the IL-6 receptor GP130 (encoded by *il6st*), will up-regulate the inflammation-involved signaling pathway, JAK/STAT. And promoting the protein level of STAT3 leads to increased tissue factor (TF) release (which is encoded by gene *f3b*), further amplifying the coagulation cascade (Park et al. 2013). Our previous study revealed that IL6-dependent JAK1/STAT3 is involved in SiNPs-induced toxicity in zebrafish embryos (Hu et al. 2016; Duan et al. 2016b). However, the full extent of the role of JAK/TF signaling pathway in inflammation–coagulation response induced by SiNPs remains to be established.

Based on the issue above, we evaluated the inflammation–coagulation response and thrombotic effects of SiNPs using *in vitro* model with endothelial cells and *in vivo* model with zebrafish. The possible biologic mechanisms were performed by transgenic zebrafish lines and *il6st* morpholinos. The usage of no observed adverse effect level (NOAEL) to assess the toxicologic response of SiNPs was also considered since the biologic effects or toxicologic response to ENMs is largely depends on dosimetry selection. It will provide persuasive evidence for nanoEHS and represent a potential target for medical therapeutics.

2. Materials and methods

2.1. Characterization of SiNPs by atomic force microscope

The preparation of SiNPs was described in our previous study (Duan et al. 2014). The size and morphology of SiNPs were also characterized by atomic force microscope (AFM) with the performance of the ScanAsyst mode, which was a peak force tapping based image optimization technique that enables creates the highest resolution AFM images using single-touch scanning. The shape, size distribution, tendency to agglomerate of SiNPs was evaluated using Dimension Icon AFM (Bruker, Fremont, CA) with

NanoScope V controller (Bruker). About 20.0 μL SiNPs were deposited onto the center of a freshly split untreated mica (V1 grade, Ted Pella Inc., Redding, CA). After that, SiNPs were adhered to the mica surface under gentle nitrogen atmosphere before imaging. The scan rate of 1.04 Hz, the scan size of 1.0 μm, the amplitude set-point of 92.35 mV, the drive amplitude of 228.58 mV, and the topology and peak force were used to determine the morphology and particle size. The particle height and the size distribution were measured by NanoScope Analysis (v. 1.80, Bruker Corporation, Germany) software.

2.2. Characterization of SiNPs by TEM and Zetasizer

Suspensions of SiNPs were dispersed by sonicator (Bioruptor UDC-200, Liege, Belgium) for 10 min prior to experimental tests. The size and shape of SiNPs was observed under a transmission electron microscope (TEM JEM-2100; JEOL Ltd., Tokyo, Japan). The hydrodynamic sizes and zeta potential of SiNPs in different mediums were detected by Zetasizer (Malvern Nano-ZS90; Malvern Instruments, Malvern, UK). The endotoxin content of SiNPs was determined using limulus amebocyte lysate (LAL) assay, with sensitivity of 0.125 EU/mL. The purity of SiNPs was measured by Inductively Coupled Plasma-Atomic Emission Spectrometry (ICP-AES) (Applied Research Laboratory, 3520, Texas, USA).

2.3. Cell culture and exposure to SiNPs

The primary human umbilical vein endothelial cells (HUVECs) were a cell culture line, which was purchased from American Type Culture Collection (ATCC, Manassas, VA). The cells were cultured in Dulbecco's Modified Eagle's Medium (DMEM) (Gibco, Carlsbad, CA) with 10% fetal bovine serum (Gibco) at humidified environment (37 °C, 5% CO_2). For *in vitro* experiments, HUVECs were seeded in six-well plates or petri dish with about 1×10^5 cells/mL for 24 h and treated with SiNPs for 24 h. Each group had five replicate wells. Controls were treated with an equivalent volume of DMEM.

2.4. Ultrastructural observation by TEM

The ultrastructural observation in SiNPs-treated endothelial cells by TEM was performed previously (Duan et al. 2013). Briefly, HUVECs treated with 50 μg/mL SiNPs for 24 h and then centrifuged for 10 min. After that, the cell samples were fixed in stationary liquid (0.1 M PBS, 2.5% glutaraldehyde, 4% paraformaldehyde), embedded in 2% agarose gel, post-fixed in 4% osmium tetroxide solution for 1 h, stained with 0.5% uranyl acetate for 1 h, dehydrated in a graded series of ethanol. After that, the samples were embedded in epoxy resin. Ultrathin sections were made and observed by TEM (JEOL JEM-2100, JEOL Ltd.).

2.5. Cell uptake and cytoskeleton structure by LSCM

After endothelial cells were attached in petri dish, the cells were cultured with ruthenium (II) hydrate ($Ru(Phen)_3^{2+}$) interior-labeled SiNPs (50 μg/mL) for cell uptake observation. HUVECs were fixed with 4% paraformaldehyde, and then washed with 0.1% Triton X-100. After that, cells were incubated with 100 nM Acti-stain™ 488 Fluorescent Phalloidin (Cytoskeleton Inc., Denver, CO) for 30 min. After that, the nucleus of HUVECs was stained with 5 μg/mL DAPI (Sigma, St. Louis, MO) for 5 min. The cellular uptake of SiNPs and cytoskeleton structure were observed under a LSCM (Leica TCS SP5, Wetzlar, Germany).

2.6. Proinflammatory and procoagulant cytokines measurement

The supernatants were collected after HUVECs exposed to SiNPs (0, 12.5, 25, 50 and 100 μg/mL) for 24 h. The levels of human interleukin IL-6, human interleukin IL-8, human monocyte chemotactic protein-1 (MCP-1), human platelet endothelial cell adhesion molecule (PECAM-1), human von Willebrand factor (vWF) were measured by ELISA kits (RayBiotech Inc., Norcross, GA) and human TF (R&D Systems, Oxford, UK) according to the manufacturer's protocols. Absorbance at 450 nm was tested by a microplate reader (Thermo Multiskan™ MK3; Thermo Fisher Scientific, Atlanta, GA).

2.7. Zebrafish husbandry and exposure to SiNPs

All zebrafish strains were provided by Hunter Biotechnology Inc (Hangzhou, China). The accreditation number from AAALAC is 001458. The husbandry

of zebrafish is in a circulating aquarium system with environmentally control (28 °C, 80% humidity). Exactly, 14-h light/10-h dark cycle was set for photoperiod. Fertilized eggs were collected by observation using a stereomicroscope (SMZ645; Nikon Corporation, Tokyo, Japan). All embryos were derived from the same spawns of eggs for statistical comparison.

2.8. Intravenous microinjection

The dosage of SiNPs was based on morphologic assessments with NOAEL in zebrafish embryos as described previously (Duan et al. 2016a). About 3 ng/nL of SiNPs was determined as the NOAEL regards to morphologic assessments by 15 indicators. SiNPs (0, 1, 3 and 6 ng/nL) were injected with 10 nL at Duct of Cuvier (DC) by microinjector (PCO-1500, Zgenebio, Taipei, Taiwan) with 30 zebrafish embryos per well for 24 h. Control group was injected with ultrapure water. For microinjection of morpholino oligo (MO), the *il6st*-MO and Con-MO were designed and bought from Gene Tools LLC (http://www.gene-tools.com). The *il6st*-MO and Con-MO were injected into embryos at one-cell stage, respectively. Gene sequences for MO are listed in Supplementary Table S1. For valid experiments, embryos were obtained only from spawns with survival rate higher than 80%.

2.9. Inflammation response in neutrophils-specific Tg(mpo:GFP) zebrafish

Neutrophils, driven by the mpo (myeloperoxidase) promoter, were observed with green fluorescence in Tg(mpo:GFP) zebrafish transgenic line after treatment with different concentrations of SiNPs for 24 h. Tg(mpo:GFP) zebrafish embryos were detected immediately under a fluorescence microscopy (AZ100, Nikon Corporation). The relative fluorescence of neutrophils was monitored and quantified by Volocity Demo 6.1.1 software (PerkinElmer, Chicago, IL).

2.10. Vascular endothelial damage in Tg(fli-1:EGFP) zebrafish embryos

Fli-1 is an early vascular endothelial marker with green fluorescence in zebrafish embryos. Tg(fli-1:EGFP) zebrafish embryos were exposed to different concentrations of SiNPs for 24 h, and examined immediately under a multi-purpose zoom fluorescence microscopy (AZ100, Nikon Corporation). Vascular endothelial damage was assessed by relative fluorescence intensity via Volocity Demo 6.1.1 software.

2.11. Hemodynamics analysis

After zebrafish embryos were exposed to different concentrations of SiNPs for 24 h, the blood flow and velocity were detected by ZebraBlood™ (v1.3.2, ViewPoint, Lyon, France) software via recording the motion of erythrocytes with tracking area. Blood flow videos were analyzed to detect changes in pixel density and combined with vessel diameter to generate a flow rate in nL/s for every frame (Parker et al. 2014).

2.12. Thrombus formation by o-dianisidine staining

o-Dianisidine staining for erythrocytes was performed as below: Briefly, after zebrafish embryos were exposed to SiNPs (0, 1, 3 and 6 ng/nL), the embryos were fixed by the 4% paraformaldehyde overnight and incubated with 0.6 mg/mL *o*-dianisidine (Sigma), staining the embryos for 10 min in the dark at room temperature. The incidence of thrombosis was observed and calculated by a stereomicroscope (SMZ645, Nikon Corporation).

2.13. Microarray and bioinformatics analysis

Microarray and bioinformatics analysis were performed as described previously (Hu et al. 2016). The mRNA expression profiling of SiNPs-treated zebrafish embryos was detected by Zebrafish Gene 1.0 ST Array (AFFY-METRIX GeneChip®, Santa Clara, CA), 59,302 gene-level of probe was setted for each chip. The microarray data from this work has been deposited in NCBI Gene Expression Omnibus (GEO) and the series accession number GSE73427. The details of Microarray data had been provided in the Supplementary material (Hu et al. 2016).

2.14. Embryos whole-mount in situ hybridization

For *in vitro* synthesis of the RNA probe, target gene fragments, such as zebrafish *jak1* and *f3b* sequences

(primers are listed in Supplementary Table S2), were cloned into pBluescript KS plasmid as the templates. Then, antisense and sense RNA probes were synthesized according to the DIG RNA labeling kit from Roche (Basel, Switzerland). Embryos were fixed with 4% paraformaldehyde overnight. Embryos were pretreated by DNase prior to starting the hybridization to remove genomic DNA pseudo-positive interference. *In situ* hybridization was performed as described previously (Hu, Zhang, and Zhang 2011).

2.15. Quantitative RT-PCR analysis

Total RNA from 50 zebrafish embryos per group was extracted by reagent (Invitrogen, Carlsbad, Canada) according to the manufacturer's protocol. Using oligo and random hexamer primers, the equal amounts of total RNA were reverse transcribed with ThermoScript reverse transcriptase. qRT-PCR reaction was run by the ABI PRISM 7500 Sequence Detection System (Applied Biosystems, Pleasonton, CA) and was performed with three biologic repeats and three duplicated repeats. The knockdown effects of MOs specific for *il6st* was verified (Supplementary Figure S1). Primers are listed in Supplementary Table S3.

2.16. Western blot analysis

Samples were blocked with 5% nonfat milk in TBST for 1 h. The PVDF membranes were incubated with glycoprotein-130 (GP130), Janus family of tyrosine kinase-1 (JAK1), signal transducers and activators of transcription-3 (STAT3; Cell Signaling Technology, Inc. Danvers, MA), TF (Biorbyt Ltd, Cambridgeshire, UK), protease-activated receptor-1 (PAR1), fibrinogen (Abcam, Cambridge, UK) (1:1000, rabbit antibodies; Abcam) overnight at 4 °C. After three times washes with TBST, the membrane were incubated with IgG secondary antibody (Abcam), followed by three further washes with TBST. Antibody-bound proteins were detected using ECL reagent (Pierce, Rockford, IL).

2.17. Statistical analysis

All statistical analysis was conducted by SPSS 18.0 software (SPSS Inc., Chicago, IL). Student's *t*-test was used for comparisons between two treatment groups. Three or more treatment groups were compared by one-way analysis of variance (ANOVA) followed by least significant difference (LSD) test. For bioinformatics analysis, the differential expression of mRNA was identified based on RVM *t*-test. Fisher's exact test was performed to select the significant pathway. Significance differences were considered at $p < 0.05$.

3. Results

3.1. Characterization of SiNPs

The interface morphology of SiNPs samples were characterized using AFM. The AFM images revealed that the SiNPs were spherical (Figure 1(A)). The spherical shape structures were visualized at high resolution from Figure 1(B). It showed high purity of SiNPs samples without contamination with micro-sized components. The particle size of SiNPs was further characterized by NanoScope analysis and the diameter size of SiNPs was 62.8 nm. According to the results of the topography, Figure 1(C) showed that SiNPs suspended in water were capable of dispersing on mica substrate without tendency for agglomerating. It should be mentioned that the SiNPs are homogeneous and any surface aggregates of the nanoparticles were not observed. The roughness analysis of NanoScope 1.8 calculated the root mean square roughness, which is the most commonly used parameter for quantitative description of surface properties. The Rq of SiNPs is 10.7 nm.

In line with AFM results, the TEM images showed that the SiNPs exhibited a near-spherical shape and were well-dispersed with average diameter of 62 nm (Figure 2(A)). The hydrodynamic sizes (Figure 2(B)) and zeta potentials (Figure 2(C)) of SiNPs in ultrapure water were $\sim 108 \pm 1$ nm and -38 ± 2 mV, respectively. No endotoxin was detected in SiNPs suspensions by LAL assay (Supplementary Table S4).

3.2. Effect of SiNPs on subcellular localization and cytoskeleton structure

The cellular uptake and subcellular localization of SiNPs in HUVECs were observed by TEM. The images of ultrastructural analysis (Figure 3(A-a,B-b)) showed that the SiNPs were internalized and induced swollen mitochondria and autophagosome in endothelial cells compared to control group. In

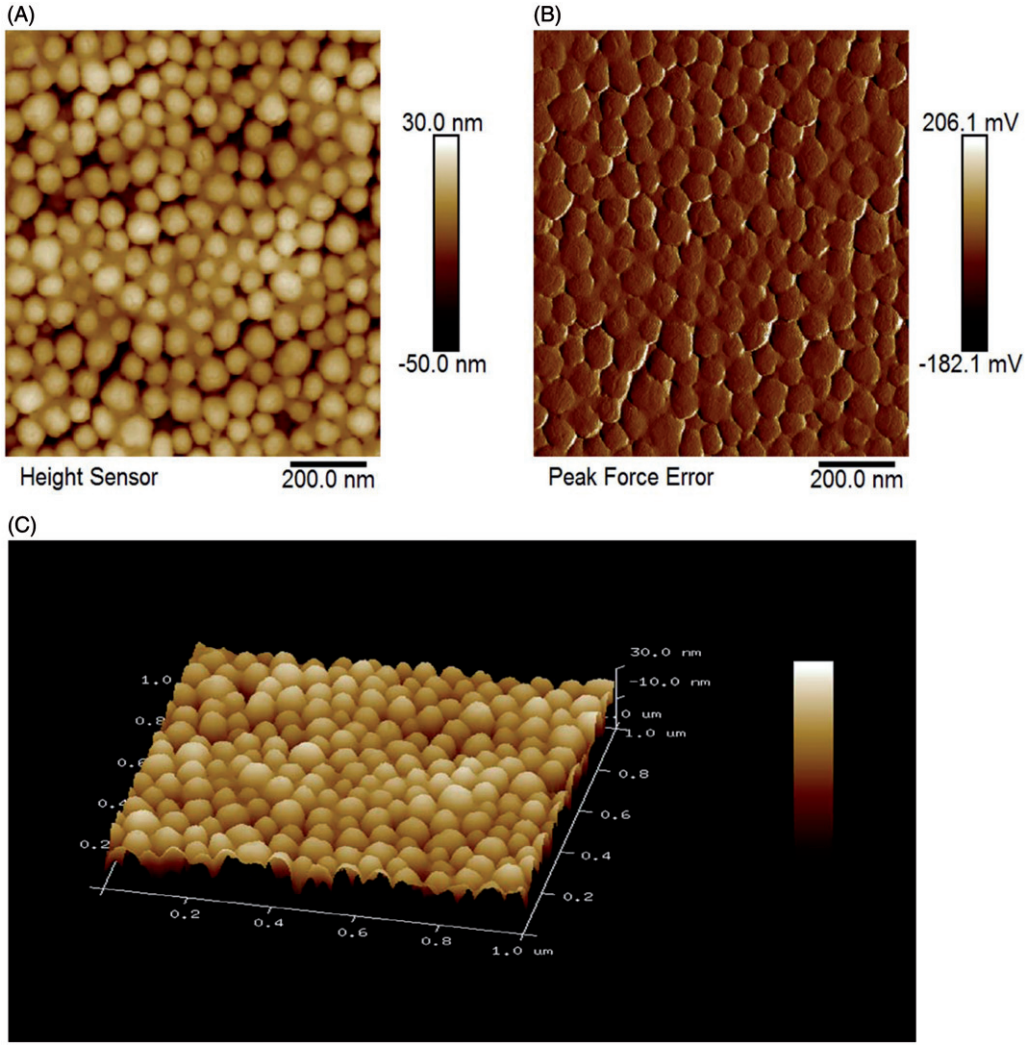

Figure 1. Characterization of SiNPs by AFM. (A) AFM height profile of SiNPs. (B) 2D peak-force error AFM scans of SiNPs. (C) 3D height image of SiNPs.

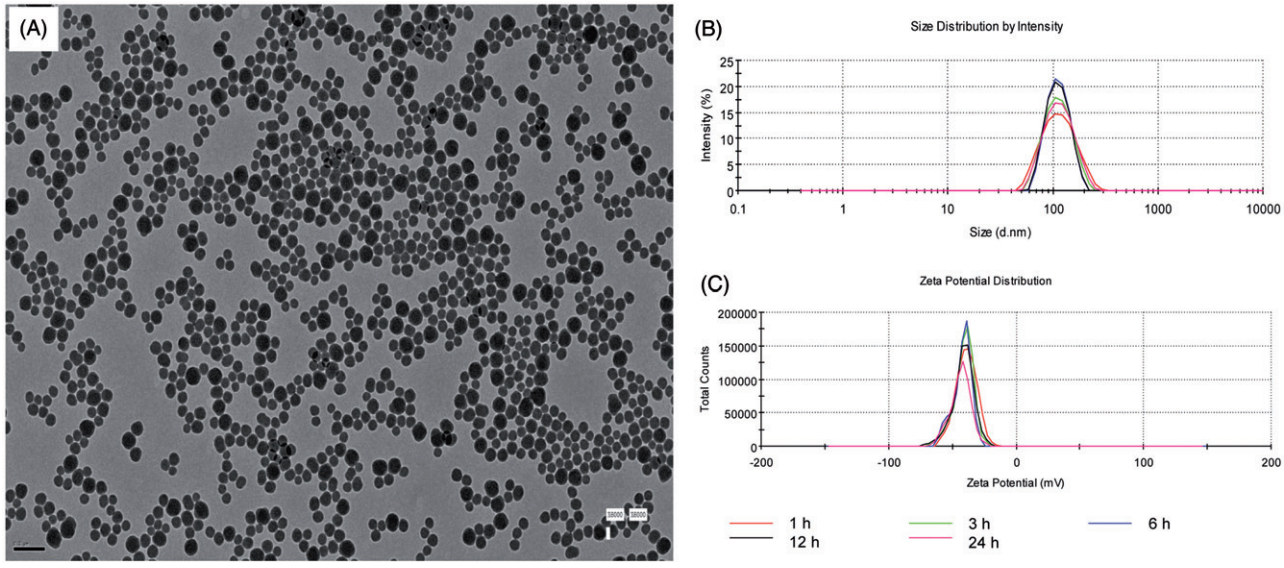

Figure 2. Characterization of SiNPs. (A) TEM of SiNPs. Scale bar, 0.2 μm. (B) Hydrodynamic sizes of SiNPs. (C) Zeta potential of SiNPs.

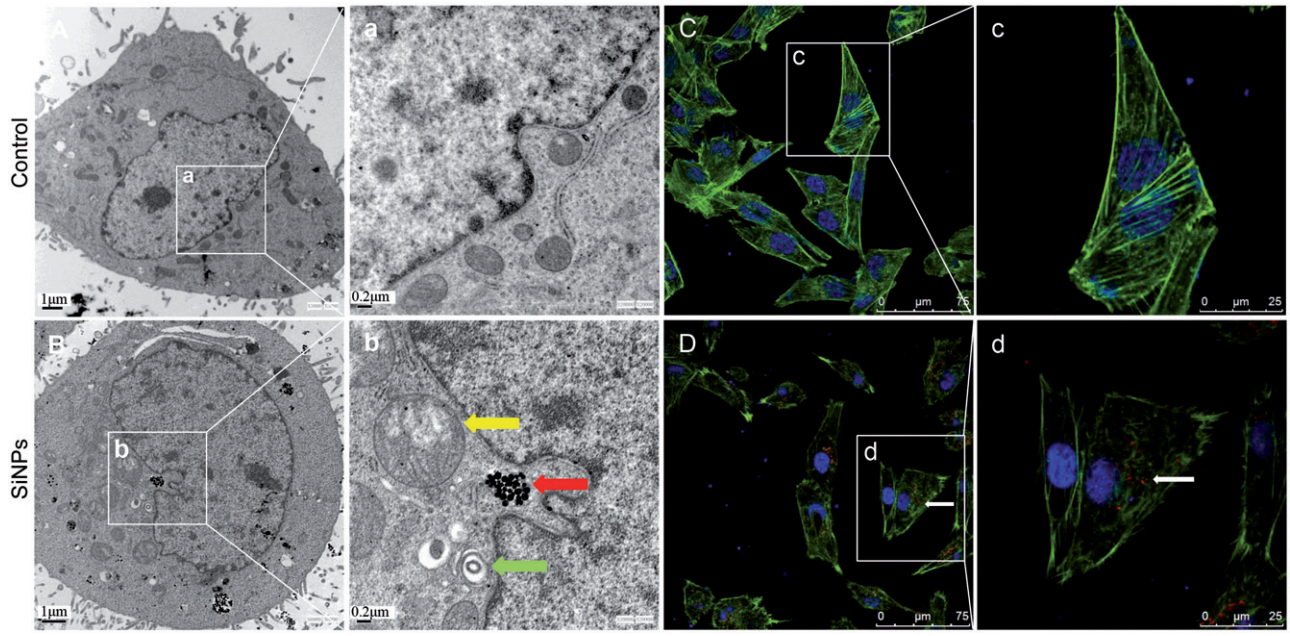

Figure 3. Ultrastructural observation and cytoskeleton structure in SiNPs-treated HUVECs. (A,C) Control group, (B,D) 50 μg/mL treated group. Yellow arrow: swollen mitochondria; red arrow: SiNPs; green arrow: autophagosome. Scale bar of TEM: (A) and (B) for 1 μm; (a) and (b) for 0.2 μm. For LSCM: F-actin (green); DAPI (blue); SiNPs (red) with white arrow.

addition, the structure of filamentous actin (F-actin) in SiNPs-treated group was further analyzed by LSCM. As shown in Figure 3(C-c), the well-organized F-actin (green fluorescent-labeled) was exhibited as thick bundles in the cytoplasm of HUVECs. Yet, in Figure 3(D-d), the fluorescent intensity of F-actin was weakened and the structure of F-actin was disrupted in HUVECs exposed to SiNPs (red fluorescent-labeled). Our data demonstrated that SiNPs could induce mitochondria damage, activate autophagy and disrupt the cytoskeleton structure in endothelial cells.

3.3. Proinflammatory and procoagulant response in endothelial cells

Since the proinflammatory and procoagulant response is a key factor for endothelial cells involved in thrombus formation, we evaluate the proinflammatory and procoagulant cytokines in SiNPs-treated HUVECs. As shown in Figure 4, the levels of IL-6, IL-8, MCP-1, PECAM-1, TF, and vWF were significantly increased in SiNPs-treated groups compared to that of control. Among them, the MCP-1 was the most sensitive cytokines response to SiNPs exposure. The significance difference appeared as early as the 12.5 μg/mL of SiNPs in endothelial cells. IL-6, IL-8, TF, and vWF were markedly elevated with the dosage higher than 25 μg/mL of SiNPs; while the release of PECAM-1 is not much sensitive to SiNPs exposure until higher than 50 μg/mL dosage. Our results indicated that SiNPs triggered the proinflammatory and procoagulant response in a dose-dependent manner, and the cytokines of proinflammatory response are more sensitive than proinflammatory response in SiNPs-treated endothelial cells.

3.4. Inflammation and vascular endothelial damage in zebrafish embryos

To evaluate the inflammatory response *in vivo*, the neutrophil recruitment and chemotaxis were monitored in caudal vein of Tg(mpo:GFP) transgenic zebrafish (Figure 5(A)). Fluorescence intensity analysis showed that the neutrophil numbers were gradually increased in a dose-dependent manner after SiNPs-treated zebrafish for 24 h (Figure 5(B)). At the highest concentration, the relative fluorescence intensity was 1.59-fold to control group. The vascular endothelial damage induced by SiNPs was further detected in Tg(fli-1:EGFP) transgenic zebrafish line. As shown in Figure 5(C), SiNPs-treated zebrafish had an inhibitory effect on the expression of vascular endothelial cells compared to control group, and the vascular pattern was disrupted

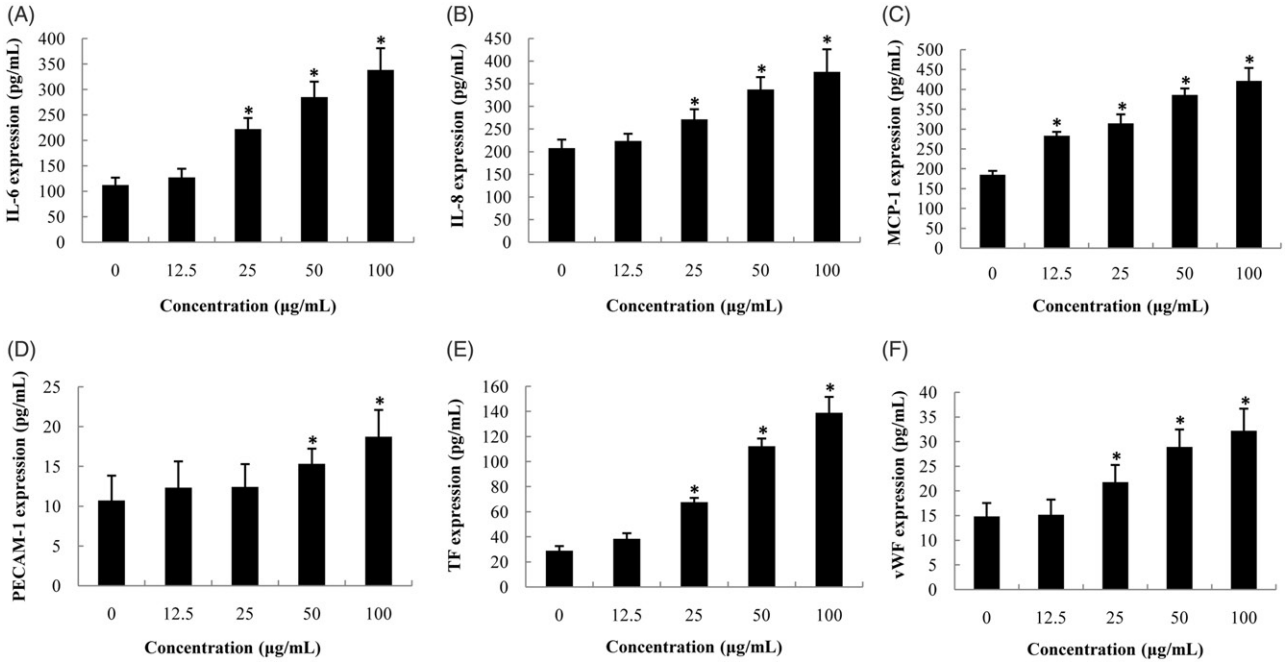

Figure 4. Effects of SiNPs on proinflammatory and procoagulant cytokines in HUVECs. (A) IL-6; (B) IL-8; (C) MCP-1; (D) PECAM-1; (E) TF; (F) vWF. Data are expressed as mean ± standard deviation from three independent experiments ($^*p < 0.05$).

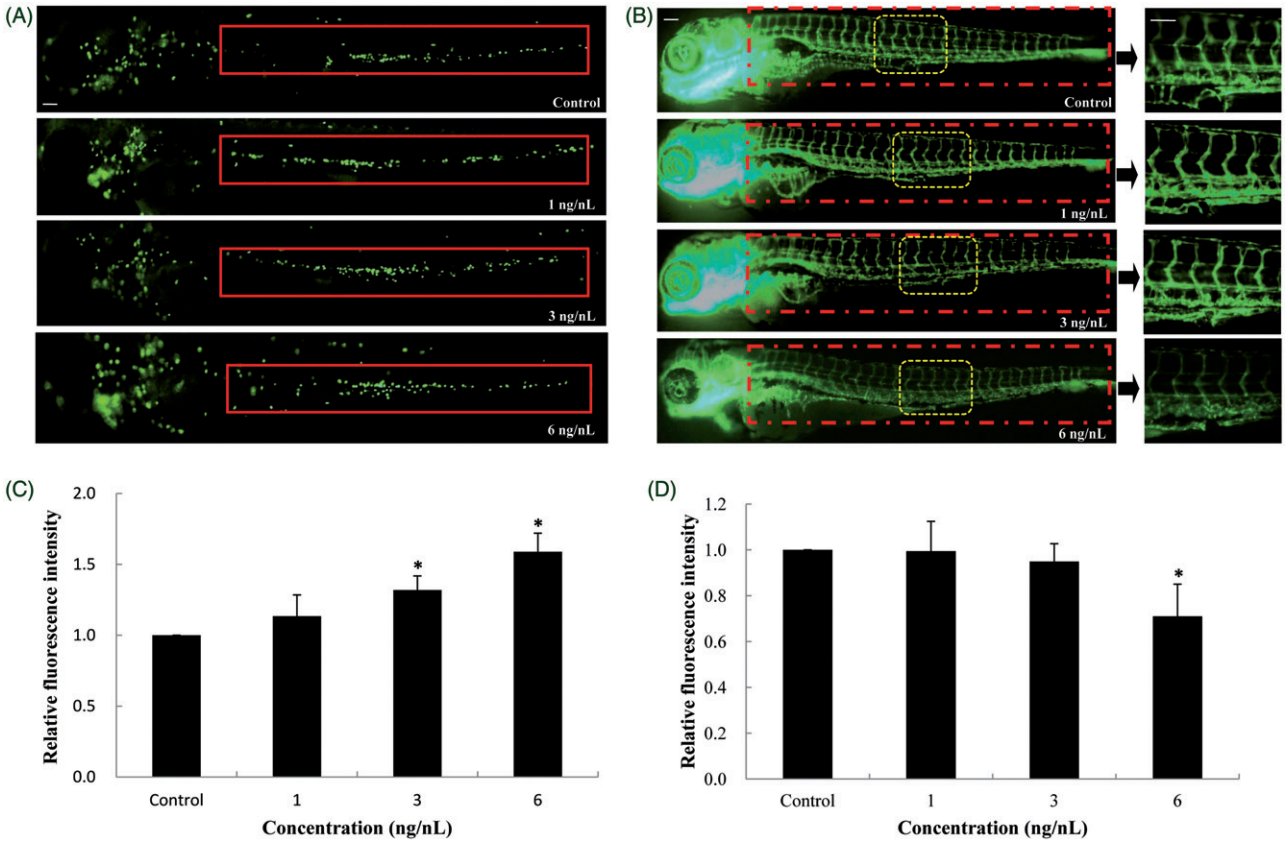

Figure 5. Inflammatory response and vascular endothelial cell dysfunction induced by SiNPs. (A,B) SiNPs increased the recruitment and chemotaxis of neutrophils in caudal vein of Tg(mpo:GFP) zebrafish. (C,D) SiNPs inhibited the expression of vascular endothelial cells in Tg(fli-1:EGFP) zebrafish. $n = 30$, data are expressed as mean ± standard deviation from three independent experiments ($^*p < 0.05$). Scale bar: 100 μm.

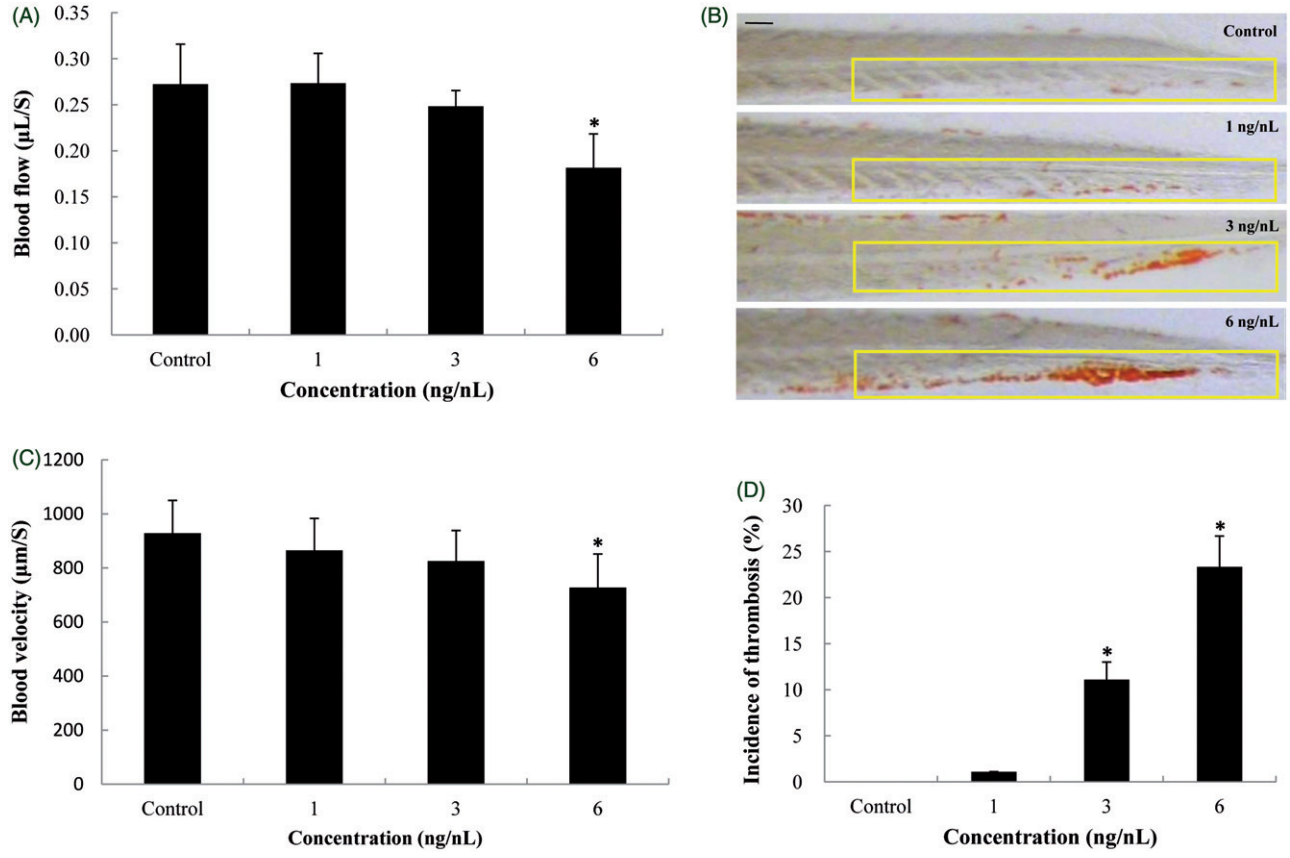

Figure 6. Hemodynamics changes and thrombus formation induced by SiNPs. (A,B) Blood flow and blood velocity were significantly decreased compared to that of control. (C,D) Erythrocytes aggregation in the caudal vein, markedly increasing the incidence of thrombosis in SiNPs-treated groups. $n = 30$, data are expressed as mean ± standard deviation from three independent experiments ($^*p < 0.05$). Scale bar: 100 μm.

obviously in the concentration that higher than NOAEL of SiNPs. In addition, the quantitative analysis showed that the relative fluorescence intensity was decreased significantly in SiNPs-treated groups compared to control (Figure 5(D)). Our data revealed that SiNPs-induced inflammatory response and vascular endothelial damage in zebrafish when the dosage is higher than NOAEL.

3.5. Hemodynamics changes and thrombotic effects in zebrafish embryos

We further evaluated the effect of SiNPs on hemodynamics and thrombus formation in zebrafish. As shown in Figure 6(A), the blood flow were gradually decreased in a dose-dependent way, and had significant changes at the highest concentration with the blood flow of 0.18 μL/S in zebrafish embryos; while the blood velocity were markedly declined compared to that of control (Figure 6(B)). Both blood flow and blood velocity decreased significantly at the SiNPs exposure level higher than NOAEL. In addition, the thrombotic effect of SiNPs on zebrafish embryos was assessed by o-dianisidine staining. Erythrocytes clearly aggregated in the caudal vein of SiNPs-treated zebrafish embryos, compared to control group (Figure 6(C)). In line with the results of *o*-dianisidine staining, Figure 6(D) showed that the incidence of thrombosis was increased markedly in SiNPs-treated groups with 26.7% increase at highest concentration. Our results demonstrated that SiNPs could induce the blood hypercoagulable state and thrombotic effects in zebrafish.

3.6. Effect of SiNPs on JAK/TF signaling pathway in zebrafish embryos

The expression of genes in JAK/TF signaling pathway was examined in zebrafish embryos according to gene chip high-throughput screening (Figure 7(A)). The related genes were verified by qRT-PCR analysis. As shown in Figure 7(B), the genes regulating inflammatory response (*il6st*, *jak1* and *stat3*) and the coagulation cascade (*f3b*, *f2r*, *fga* and *fgb*) were

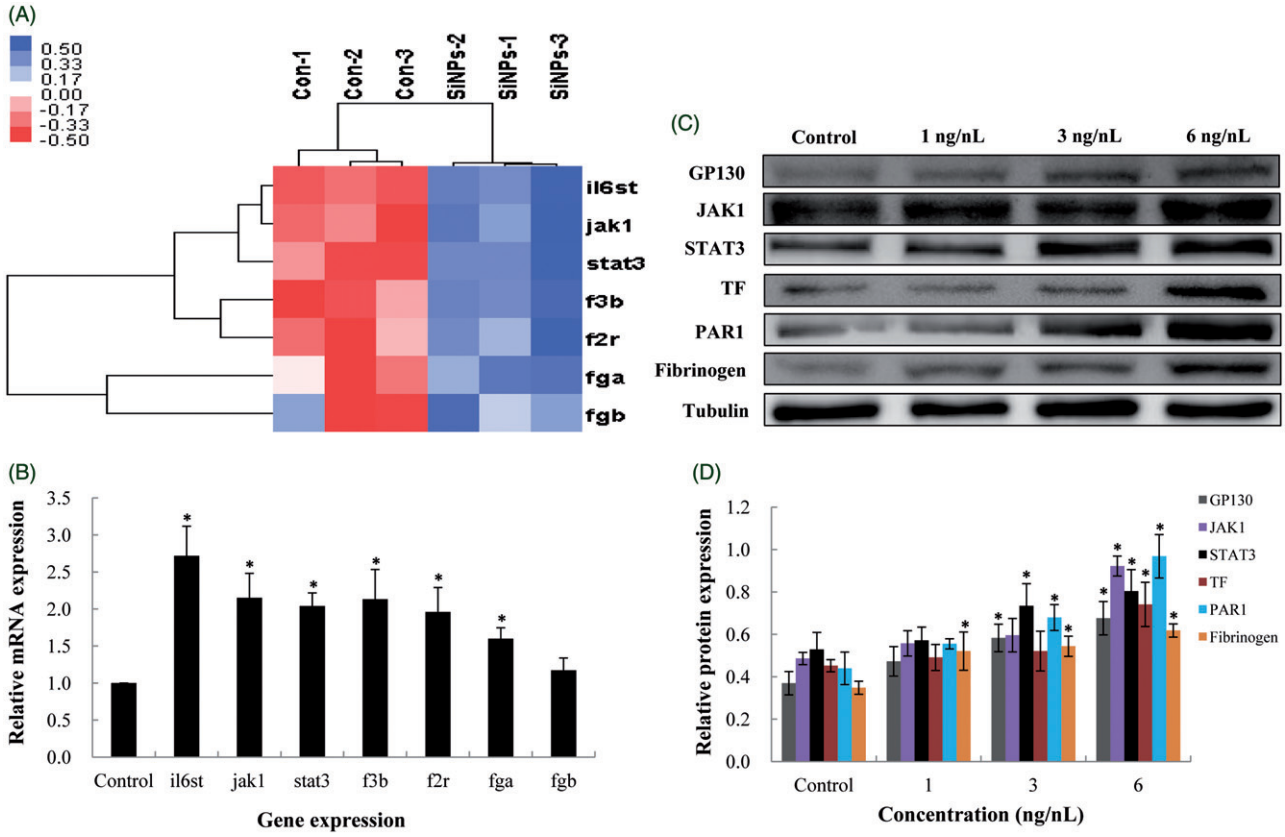

Figure 7. Effect of SiNPs on the JAK1/TF signaling pathway. (A) Heat map from microarray analysis of inflammation–coagulation cascade related genes. (B) qRT-PCR analysis showed that the genes involved in inflammation–coagulation response. (C,D) SiNPs activated the JAK1/TF signaling pathway in a dose-dependent manner. $n = 50$, data are expressed as mean ± standard deviation from three independent experiments ($^*p < 0.05$).

decreased following SiNPs treatment. In addition, the expression of inflammation–coagulation response related proteins, such as GP130, JAK1, STAT3, TF, PAR1 and fibrinogen were significantly down-regulated in a dose-dependent manner (Figure 7(C,D)). It was worth to mention that, the fibrinogen is a gold indicator for thrombus formation, indicating that SiNPs had a thrombotic effect on zebrafish.

In addition, the JAK1/TF pathway was further verified by MO. *il6st* was knockdown to analyze the expression of JAK1 and TF induced by SiNPs *in situ*. Results from the whole-mount *in situ* hybridization analysis showed that the expression pattern of *jak1* in zebrafish embryos was only otic capsule; while the *f3b* expression pattern was hindbrain and otic capsule (Figure 8(A)). As shown in Figure 8(B), the quantitative analysis demonstrated that either *jak1* or *f3b* expression in *il6st*-MO group was similar to Con-MO group, respectively. Both *jak1* and *f3b* expression in Con-MO treated with SiNPs groups were significantly elevated; whereas the expression *jak1* and *f3b* were attenuated in *il6st*-MO treated with SiNPs groups. A schematic model of the molecular mechanisms involved in this study was presented in Figure 8(C). Taken together, our data showed that SiNPs could induce inflammation–coagulation response and thrombotic effects via JAK/TF signaling pathway in zebrafish embryos.

4. Discussion

Currently, NanoEHS required us to understand the properties of the engineered nanomaterials (ENMs) that are responsible for the toxicologic response, since it is benefit for designing safety ENMs (Nel et al. 2009). This study was built on our previous work to verified and elaborate on inflammation–-coagulation response triggered by SiNPs in endothelial cells and in zebrafish embryos. We revealed that the JAK1/TF signaling pathway is responsible for thrombotic effects induced by SiNPs. It could be helpful to understand the cardiovascular toxicity induced by SiNPs, also it could be considered for

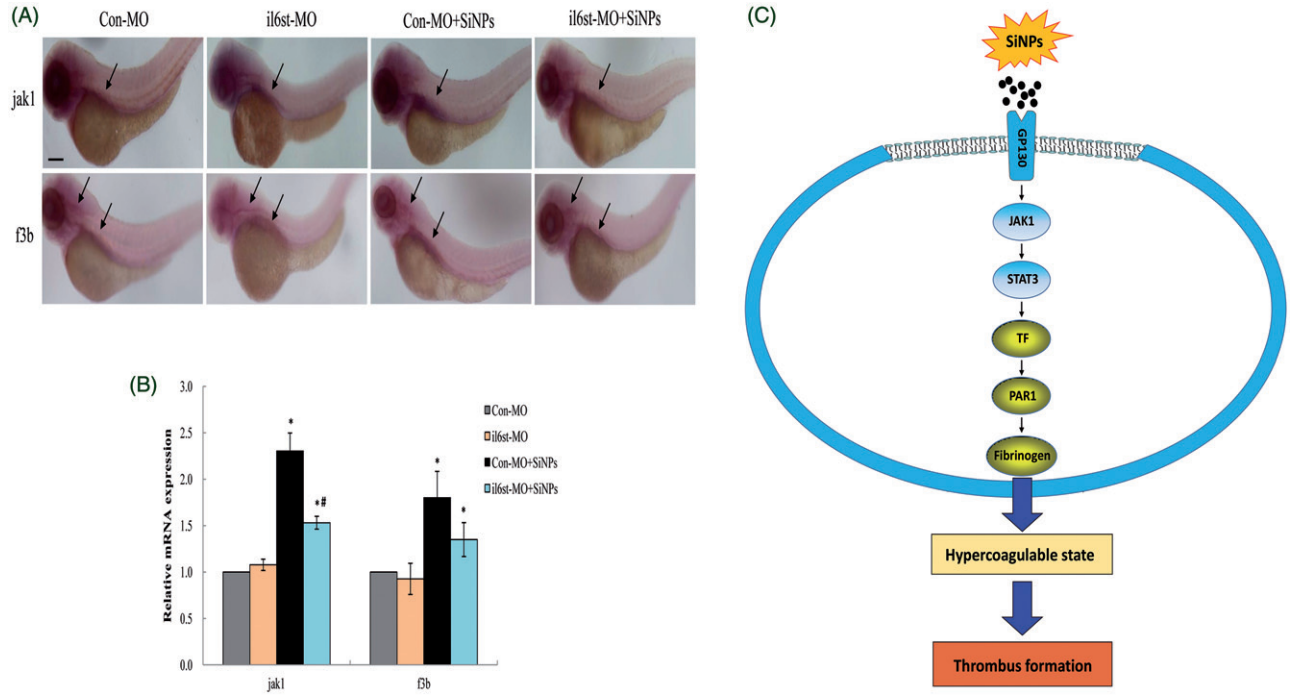

Figure 8. Knockdown of *il6st* declined the expression of *jak1* and *f3b* induced by SiNPs. (A) Whole-mount *in situ* hybridization analysis showed that the expression pattern of *jak1* in zebrafish embryos was only otic capsule; while the *f3b* expression pattern was hindbrain and otic capsule. (B) Quantitative analysis demonstrated that the expression *jak1* and *f3b* induced by SiNPs were decreased in *il6st*-MO group compared to Con-MO group. (C) A schematic model of the molecular mechanisms involved in this study was presented. Signaling molecules with blue color denote as inflammation-related proteins; while gold color denote as coagulation-related proteins. $n = 50$, data are expressed as mean ± standard deviation from three independent experiments ($^{*}p < 0.05$).

reducing the hazardous effects of nano-based products in biomedicine fields.

Detailed characterization of ENMs is considered as a guarantee for performing toxicity research (DeLoid et al. 2017). In this study, AFM, TEM, DSL, and ICP-AES were utilized to test the features of SiNPs. The endotoxin content of SiNPs was determined by LAL assay. Our data showed that the SiNPs used in our study exhibited good monodispersity and favorable dispersibility (Figures 1 and 2, and Supplementary Table S2), which are conducive to the following toxicologic experiments. For *in vitro* study, our data found that SiNPs-induced mitochondria damage, activate autophagy and disrupt the cytoskeleton structure in endothelial cells (Figure 3). Autophagy and mitochondria damage are emerged as new mechanisms of nanomaterial toxicity (Stern, Adiseshaiah, and Crist 2012). When SiNPs was uptake by endothelial cells, it is unavoidable to contact with the cytoskeleton structure, F-actin. SiNPs may cause the changes of actin states (polymerization or depolymerization), because as far as we know, the F-actin is the most favorable proteins that could bound with various size of particles (Ehrenberg and McGrath 2005). In recently, there are a growing body of literatures reported that the actin remodeling of cytoskeleton organization is closely involved in autophagy (Mostowy and Cossart 2011). Therefore, more studies are encouraged to explore the possible mechanisms between cytoskeleton and autophagy triggered by ENMs.

Oxidative stress is a widely accepted mechanism for nanoparticle-induced toxicity *in vivo* and *in vitro* (Khatri et al. 2013). Previously, we found that the SiNPs triggered ROS generation in zebrafish embryos (Duan et al. 2016a). SiNPs have the capacity to generate hydroxyl radicals ($^{\bullet}$OH) that would promote cellular oxidative stress and inflammatory response, and potentially instigating widespread effects systemically (Mendoza et al. 2014). Here, we evaluated the proinflammatory-procoagulant response *in vitro* and *in vivo*. Using vascular endothelial cell model, we found that the release of proinflammatory cytokines (IL-6, IL-8 and MCP-1) and procoagulant cytokines (PECAM-1, TF and vWF), were significantly elevated in a dose-dependent

manner (Figure 4). It was worth noting that, after vascular endothelial cells was stimulated by SiNPs, the vessel endothelium wall will be switched into a proinflammatory and procoagulant status. The coagulatory protein vWF plays as a mediator for platelet adhesion to the endothelium, eventually turn into thrombus formation in living body (Bauer et al. 2011).

Currently, zebrafish is becoming a popular model for NanoEHS study. Using two transgenetic zebrafish lines, Tg(mpo:GFP) and Tg(fli-1:EGFP), we demonstrated that the vascular endothelial damage accompanied by neutrophil recruitment were detected in the cardiac region of SiNPs-treated groups (Figure 5). MPO is a specific marker expressed only in neutrophil granules, which could reflect the inflammatory response in zebrafish (Bennett et al. 2001). In response to inflammation, the neutrophils migrate from the circulation to injured tissues. Excessive oxidative stress and inflammatory responses with in circulation system induce vascular endothelial damage. Tg(fli-1:EGFP) transgenic zebrafish with green-fluorescent vascular structure, is a useful model to assess the vascular appearance and patterning (Rizvi, Mehta, and Oyekan 2013). So far, only a few studies have addressed the vascular patterning caused by nanoparticles. Quantum dots (QDs) had been shown to induce abnormal vascular patterns in Fli-1 transgenic zebrafish, such as vascular junction, bifurcation, crossing and high fluorescent expression (Zhang et al. 2012). Although in contrast to other reports, our study found that SiNPs had an inhibitory effect on vascular endothelial cell, more research is needed on this issue.

The transparent embryos of albino zebrafish line are a useful model to visualize the hemodynamics and thrombus formation in a living organism. Given that the lower blood flow and velocity observed in SiNPs-exposed zebrafish might impact on hemodynamics, we also analyzed thrombus formation in zebrafish embryos using *o*-dianisidine staining. Since the erythrocyte was up to 90% of all cell types in blood components, our results revealed that SiNPs triggered blood hypercoagulable state and thrombotic effects in zebrafish embryos (Figure 6). A marked erythrocytes aggregation was observed in SiNPs-treated groups in a dose-dependent manner. We addressed the underlying mechanism of this phenomenon using the KEGG database and microarray analysis, and verified that the SiNPs-induced JAK1/TF signaling pathway by *il6st* knockdown (Figures 7 and 8). The JAK signaling pathway is a critical to regulator inflammation, angiogenesis, vascular cell growth, immune response and other cellular processes. TF can regulate protease-activated receptor (PAR) signaling, directly or indirectly through thrombin generation (Reinhardt et al. 2012). Under pathologic conditions, TF is expressed on the membrane surface of almost all the blood cells and vascular endothelial cells, providing a widespread trigger for the coagulation cascade, resulting in disseminated intravascular coagulation (DIC) or thrombosis (Bode and Mackman 2014). Interactions between TF and PAR1 (encoded by *f2r*), also play an important role in platelet function and thrombus formation (Mackman 2009). It has been reported that knocked down the gene *f2r* caused a bleeding phenotype in zebrafish embryos, suggesting that *f2r* might enhance the blood coagulation (Ellertsdottir et al. 2012). In a recent study, hemorrhaging was also observed in *fga* mutation zebrafish model (Fish, Di Sanza, and Neerman-Arbez 2014). The fibrinogen is encoded by a cluster of three genes *fga*, *fgb* and *fgg* in zebrafish (Fish et al. 2011). Fibrinogen as the precursor to fibrins is one of the most abundant coagulation factors, which can be rapidly transformed into fibrin monomer and insoluble fibrin polymer, making a prominent contribution to coagulation cascade and thrombus formation (Ryu et al. 2015). Previously, our study found that SiNPs increased the fibrinogen level detected by blood samples in rats, but far from understanding the molecular mechanisms (Jiang et al. 2015). In this study, we elucidate the underlying mechanisms of SiNPs on the inflammation–coagulation response and thrombotic effects.

5. Conclusions

In summary, our study found that SiNPs triggered inflammation–coagulation response and thrombotic effects in zebrafish embryos; SiNPs improved the release of proinflammatory and procoagulant cytokines in endothelial cells. We revealed that the JAK1/TF signaling pathway was responsible for SiNPs-induced thrombus formation *in vivo*. Besides characterization of ENMs, The dosimetry selection is

also a key factor for biologic effects or toxicologic response to ENMs. Thus, the usage of NOAEL to assess the toxicologic response of ENMs should also be fully considered. In turn, it will be helpful in safe-by-design strategies for improving nano-related products.

Acknowledgements

The authors thank Weiping Tang from CNKINGBIO for bio-informatics assistance, Hongcui Liu and Zijian Zhuo from Hunter Biotechnology, Inc., for technical support.

Disclosure statement

No potential conflict of interest was reported by the authors.

Funding

This work was supported by National Natural Science Foundation of China [no. 81502830, 81773462] and Beijing Municipal Natural Science Foundation [7172027]. M.R.M. is supported by the British Heart Foundation [SP/15/8/31575].

ORCID

Mark R. Miller http://orcid.org/0000-0002-7078-597X

References

Bauer, A. T., E. A. Strozyk, C. Gorzelanny, C. Westerhausen, A. Desch, M. F. Schneider, and S. W. Schneider. 2011. "Cytotoxicity of Silica Nanoparticles through Exocytosis of von Willebrand Factor and Necrotic Cell Death in Primary Human Endothelial Cells." *Biomaterials* 32 (33): 8385–8393. doi:10.1016/j.biomaterials.2011.07.078.

Benezra, M., O. Penate-Medina, P. B. Zanzonico, D. Schaer, H. Ow, A. Burns, E. Destanchina, et al. 2011. "Multimodal Silica Nanoparticles Are Effective Cancer-Targeted Probes in a Model of Human Melanoma." *Journal of Clinical Investigation* 121 (7): 2768–2780. doi:10.1172/JCI45600.

Bennett, C. M., J. P. Kanki, J. Rhodes, T. X. Liu, B. H. Paw, M. W. Kieran, D. M. Langenau, et al. 2001. "Myelopoiesis in the Zebrafish, Danio rerio." *Blood* 98: 643–651.

Bode, M., and N. Mackman. 2014. "Regulation of Tissue Factor Gene Expression in Monocytes and Endothelial Cells: Thromboxane A2 as a New Player." *Vascular Pharmacology* 62 (2): 57–62. doi:10.1016/j.vph.2014.05.005

Deloid, G. M., J. M. Cohen, G. Pyrgiotakis, and P. Demokritou. 2017. "Preparation, Characterization, and In Vitro Dosimetry of Dispersed, Engineered Nanomaterials." *Nature Protocols* 12 (2): 355–371. doi:10.1038/nprot.2016.172.

Duan, J., Y. Yu, Y. Li, Y. Li, H. Liu, L. Jing, M. Yang, J. Wang, C. Li, and Z. Sun. 2016. "Low-Dose Exposure of Silica Nanoparticles Induces Cardiac Dysfunction via Neutrophil-Mediated Inflammation and Cardiac Contraction in Zebrafish Embryos." *Nanotoxicology* 10 (5): 575–585. doi:10.3109/17435390.2015.1102981.

Duan, J., Y. Yu, Y. Li, Y. Wang, and Z. Sun. 2016. "Inflammatory Response and Blood Hypercoagulable State Induced by Low Level Co-Exposure with Silica Nanoparticles and Benzo[a]Pyrene in Zebrafish (Danio rerio) Embryos." *Chemosphere* 151: 152–162. doi:10.1016/j.chemosphere.2016.02.079.

Duan, J., Y. Yu, Y. Li, Y. Yu, and Z. Sun. 2013. "Cardiovascular Toxicity Evaluation of Silica Nanoparticles in Endothelial Cells and Zebrafish Model." *Biomaterials* 34 (23): 5853–5862. doi:10.1016/j.biomaterials.2013.04.032.

Duan, J., Y. Yu, Y. Yu, Y. Li, P. Huang, X. Zhou, S. Peng, and Z. Sun. 2014. "Silica Nanoparticles Enhance Autophagic Activity, Disturb Endothelial Cell Homeostasis and Impair Angiogenesis." *Particle and Fibre Toxicology* 11 (1): 50. doi:10.1186/s12989-014-0050-8.

Ehrenberg, M., and J. L. Mcgrath. 2005. "Binding between Particles and Proteins in Extracts: Implications for Microrheology and Toxicity." *Acta Biomaterialia* 1 (3): 305–315. doi:10.1016/j.actbio.2005.02.002

Ellertsdottir, E.,. P. R. Berthold, M. Bouzaffour, P. Dufourcq, V. Trayer, C. Gauron, S. Vriz, M. Affolter, and C. Rampon. 2012. "Developmental Role of Zebrafish Protease-Activated Receptor 1 (PAR1) in the Cardio-Vascular System." *PLoS One* 7 (7): e42131. doi:10.1371/journal.pone.0042131.

Etheridge, M. L., S. A. Campbell, A. G. Erdman, C. L. Haynes, S. M. Wolf, and J. Mccullough. 2013. "The Big Picture on Nanomedicine: The State of Investigational and Approved Nanomedicine Products." *Nanomedicine* 9 (1): 1–14. doi:10.1016/j.nano.2012.05.013.

Fako, V. E., and D. Y. Furgeson. 2009. "Zebrafish as a Correlative and Predictive Model for Assessing Biomaterial Nanotoxicity." *Advanced Drug Delivery Reviews* 61 (6): 478–486. doi:10.1016/j.addr.2009.03.008.

Fang, Y., V. Gupta, R. Karra, J. E. Holdway, K. Kikuchi, and K. D. Poss. 2013. "Translational Profiling of Cardiomyocytes Identifies an Early Jak1/Stat3 Injury Response Required for Zebrafish Heart Regeneration." *Proceedings of the National Academy of Sciences of the United States of America* 110 (33): 13416–13421. doi:10.1073/pnas.1309810110.

Fish, R. J., C. DI Sanza, and M. Neerman-Arbez. 2014. "Targeted Mutation of Zebrafish Fga Models Human Congenital Afibrinogenemia." *Blood* 123 (14): 2278–2281. doi:10.1182/blood-2013-12-547182.

Fish, R. J., S. Vorjohann, F. Bena, A. Fort, and M. Neerman-Arbez. 2011. "Developmental Expression and Organisation of Fibrinogen Genes in the Zebrafish." *Thrombosis and Haemostasis* 107 (1): 158–166. doi:10.1160/TH11-04-0221.

Gabizon, A.,. M. Bradbury, U. Prabhakar, W. Zamboni, S. Libutti, and P. Grodzinski. 2014. "Cancer Nanomedicines: Closing the Translational Gap." *Lancet* 384 (9961): 2175–2176. doi:10.1016/S0140-6736(14)61457-4.

Hansen, S. F., E. S. Michelson, A. Kamper, P. Borling, F. Stuer-Lauridsen, and A. Baun. 2008. "Categorization Framework to Aid Exposure Assessment of Nanomaterials in Consumer Products." *Ecotoxicology* 17 (5): 438–447. doi:10.1007/s10646-008-0210-4.

Hicken, C. E., T. L. Linbo, D. H. Baldwin, M. L. Willis, M. S. Myers, L. Holland, M. Larsen, et al. 2011. "Sublethal Exposure to Crude Oil during Embryonic Development Alters Cardiac Morphology and Reduces Aerobic Capacity in Adult Fish." *Proceedings of the National Academy of Sciences of the United States of America* 108 (17): 7086–7090. doi:10.1073/pnas.1019031108.

Hu, H., Q. Li, L. Jiang, Y. Zou, J. Duan, and Z. Sun. 2016. "Genome-Wide Transcriptional Analysis of Silica Nanoparticles-Induced Toxicity in Zebrafish Embryos." *Toxicology Research* 5 (2): 609–620. doi:10.1039/C5TX00383K

Hu, Z., J. Zhang, and Q. Zhang. 2011. "Expression Pattern and Functions of Autophagy-Related Gene atg5 in Zebrafish Organogenesis." *Autophagy* 7 (12): 1514–1527. doi:10.4161/auto.7.12.18040.

Ilinskaya, A. N., and M. A. Dobrovolskaia. 2013. "Nanoparticles and the Blood Coagulation System. Part I: Benefits of Nanotechnology." *Nanomedicine* 8 (5): 773–784. doi:10.2217/nnm.13.48.

Jiang, L., Y. Li, Y. Li, C. Guo, Y. Yu, Y. Zou, Y. Yang, et al. 2015. "Silica Nanoparticles Induced the Pre-Thrombotic State in Rats via Activation of Coagulation Factor XII and the JNK-NF-κB/AP-1 Pathway." *Toxicology Research* 4 (6): 1453–1464. doi:10.1039/C5TX00118H.

Jun, E. A., K. M. Lim, K. Kim, O. N. Bae, J. Y. Noh, K. H. Chung, and J. H. Chung. 2011. "Silver Nanoparticles Enhance Thrombus Formation through Increased Platelet Aggregation and Procoagulant Activity." *Nanotoxicology* 5 (2): 157–167. doi:10.3109/17435390.2010.506250.

Khatri, M., D. Bello, P. Gaines, J. Martin, A. K. Pal, R. Gore, and S. Woskie. 2013. "Nanoparticles from Photocopiers Induce Oxidative Stress and Upper Respiratory Tract Inflammation in Healthy Volunteers." *Nanotoxicology* 7 (5): 1014–1027. doi:10.3109/17435390.2012.691998.

Mackman, N. 2009. "The Many Faces of Tissue Factor." *Journal of Thrombosis and Haemostasis* 7(Suppl. 1): 136–139. doi:10.1111/j.1538-7836.2009.03368.x.

Maynard, A. D. 2014. "Old Materials, New Challenges?" *Nature Nanotechnology* 9 (9): 658–659. doi:10.1038/nnano.2014.196.

Mendoza, A., J. A. Torres-Hernandez, J. G. Ault, J. H. Pedersen-Lane, D. Gao, and D. A. Lawrence. 2014. "Silica Nanoparticles Induce Oxidative Stress and Inflammation of Human Peripheral Blood Mononuclear Cells." *Cell Stress Chaperones* 19 (6): 777–790. doi:10.1007/s12192-014-0502-y.

Mostowy, S., and P. Cossart. 2011. "Autophagy and the Cytoskeleton New Links Revealed by Intracellular Pathogens." *Autophagy* 7 (7): 780–782. doi:10.4161/auto.7.7.15593.

Murray, P. J. 2007. "The JAK-STAT Signaling Pathway: Input and Output Integration." *Journal of Immunology* 178 (5): 2623–2629. doi:10.4049/jimmunol.178.5.2623.

Nel, A. E., C. J. Brinker, W. J. Parak, J. I. Zink, W. C. W. Chan, K. E. Pinkerton, T. Xia, D. R. Baer, M. C. Hersam, and P. S. Weiss. 2015. "Where Are We Heading in Nanotechnology Environmental Health and Safety and Materials Characterization?" *ACS Nano* 9 (6): 5627–5630. doi:10.1021/acsnano.5b03496.

Nel, A. E., L. Madler, D. Velegol, T. Xia, E. M. V. Hoek, P. Somasundaran, F. Klaessig, V. Castranova, and M. Thompson. 2009. "Understanding Biophysicochemical Interactions at the Nano-Bio Interface." *Nature Materials* 8 (7): 543–557. doi:10.1038/nmat2442.

OECD. 2010. "Series on the Safety of Manufactured Nanomaterials. No. 27-ENV/JM/MONO(2010)46. France. Accessed 30 December 2017. http://www.oecd.org/science/nanosafety/.

Park, D. W., J. H. Lyu, J. S. Kim, H. Chin, Y. S. Bae, and S. H. Baek. 2013. "Role of JAK2-STAT3 in TLR2-Mediated Tissue Factor Expression." *Journal of Cellular Biochemistry* 114 (6): 1315–1321. doi:10.1002/jcb.24472.

Parker, T., P. A. Libourel, M. J. Hetheridge, R. I. Cumming, T. P. Sutcliffe, A. C. Goonesinghe, J. S. Ball, S. F. Owen, Y. Chomis, and M. J. Winter. 2014. "A Multi-Endpoint In Vivo Larval Zebrafish (*Danio rerio*) Model for the Assessment of Integrated Cardiovascular Function." *Journal of Pharmacological and Toxicological Methods* 69 (1): 30–38. doi:10.1016/j.vascn.2013.10.002.

Rao, A. N., N. M. Kazzaz, and J. S. Knight. 2015. "Do Neutrophil Extracellular Traps Contribute to the Heightened Risk of Thrombosis in Inflammatory Diseases?" *World Journal of Cardiology* 7 (12): 829–842. doi:10.4330/wjc.v7.i12.829.

Reinhardt, C., M. Bergentall, T. U. Greiner, F. Schaffner, G. Ostergren-Lunden, L. C. Petersen, W. Ruf, and F. Backhed. 2012. "Tissue Factor and PAR1 Promote Microbiota-Induced Intestinal Vascular Remodelling." *Nature* 483 (7391): 627–631. doi:10.1038/nature10893.

Rizvi, Y. Q., C. S. Mehta, and A. Oyekan. 2013. "Interactions of PPAR-Alpha and Adenosine Receptors in Hypoxia-Induced Angiogenesis." *Vascular Pharmacology* 59 (5–6): 144–151. doi:10. 1016/j.vph.2013.09.001.

Ryu, J. K., M. A. Petersen, S. G. Murray, K. M. Baeten, A. Meyer-Franke, J. P. Chan, E. Vagena, et al. 2015. "Blood Coagulation Protein Fibrinogen Promotes Autoimmunity and Demyelination via Chemokine Release and Antigen Presentation." *Nature Communications* 6 (1): 8164. doi:10.1038/ncomms9164.

Solayar, G. N., and F. J. Shannon. 2014. "Thromboprophylaxis and Orthopaedic Surgery: Options and Current Guidelines." *Malaysian Journal of Medical Sciences* 21: 71–77.

Stern, S. T., P. P. Adiseshaiah, and R. M. Crist. 2012. "Autophagy and Lysosomal Dysfunction as Emerging Mechanisms of Nanomaterial Toxicity." *Particle and Fibre Toxicology* 9 (1): 20. doi:10.1186/1743-8977-9-20.

Weyand, A. C., and J. A. Shavit. 2014. "Zebrafish as a Model System for the Study of Hemostasis and Thrombosis."

Current Opinion in Hematology 21 (5): 418–422. doi:10.1097/MOH.0000000000000075.

Xu, R., G. Zhang, J. Mai, X. Deng, V. Segura-Ibarra, S. Wu, J. Shen, et al. 2016. "An Injectable Nanoparticle Generator Enhances Delivery of Cancer Therapeutics." *Nature Biotechnology* 34 (4): 414–418. doi:10.1038/nbt.3506.

Yoshida, T., Y. Yoshioka, S. Tochigi, T. Hirai, M. Uji, K. Ichihashi, K. Nagano, et al. 2013. "Intranasal Exposure to Amorphous Nanosilica Particles Could Activate Intrinsic Coagulation Cascade and Platelets in Mice." *Particle and Fibre Toxicology* 10 (1): 41. doi:10.1186/1743-8977-10-41.

Zhang, W., K. Lin, X. Sun, Q. Dong, C. Huang, H. Wang, M. Guo, and X. Cui. 2012. "Toxicological Effect of MPA-CdSe QDs Exposure on Zebrafish Embryo and Larvae." *Chemosphere* 89 (1): 52–59. doi:10.1016/j.chemosphere.2012.04.012.